

Mechanical and Thermo-Physical Properties of High-Density Polyethylene Modified with Talc

Adib Kalantar Mehrjerdi,¹ Bijan Adl-Zarrabi,² Sung-Woo Cho,¹ Mikael Skrifvars¹

¹School of Engineering, University of Borås, SE-501 90 Borås, Sweden

²Civil and Environmental Engineering, Chalmers University of Technology, SE-412 96 Gothenburg, Sweden

Correspondence to: M. Skrifvars (E-mail: mikael.skrifvars@hb.se)

ABSTRACT: The aim of this study was to examine the physical, mechanical, and thermo-physical properties of high-density polyethylene (HDPE) modified with talc. Different weight fractions of talc (up to 35 wt %) were compounded with an HDPE matrix containing 2.5 wt % of carbon black (CB) in a twin-screw compounder. The composites were then processed by injection moulding to obtain specimens for testing. The results indicate that CB causes a significant decrease in the toughness, while talc not only enhances the thermal conductivity and thermo-physical properties of the composites but can also play a role in compensating for the negative effects of CB on impact resistance. The experimental data show that the presence of CB reduces the impact resistance of HDPE by up to 34%, while addition of up to 8 wt % talc can return this value to close to that of pure HDPE. No significant effect on the composite tensile yield and fracture strength was observed for either component at all concentrations. The thermal conductivity, thermal diffusivity, and specific density values of the composites increased almost linearly, but the increase in moisture absorption in the long term showed nonlinear behavior in the concentration range of the experiment. © 2013 Wiley Periodicals, Inc. *J. Appl. Polym. Sci.* 129: 2128–2138, 2013

KEYWORDS: polyolefins; thermal properties; blends; composites; differential scanning calorimetry

Received 19 June 2012; accepted 13 December 2012; published online 13 January 2013

DOI: 10.1002/app.38945

INTRODUCTION

Modern society has been influenced to a great degree by polymer technology. In fact, today we could not imagine living without polymers and polymer composites. Also, researchers and practitioners are attempting to develop new materials by reducing the size of material constituents to the nanoscopic scale, and by different types of compositions to achieve a wide variety of properties. Ever since the polymer industry developed, significant efforts have been made to improve the properties of polymers according to market needs. Most properties of polymers can be enhanced using reinforcing agents, additives, and fillers to fulfil material requirements for very specific applications. In many cases, synergistic effects can also be seen when two or more fillers are used at the same time.

By adding fillers and particles to polymers, the mechanical,^{1,2} electrical, and thermal properties,^{3,4} and also their UV stability, can be improved.⁵ Many particles have been used, such as metals, carbon, glass fiber, and ceramic, each of which can give different qualities and properties for the intended end use, so it is therefore important to fully understand the effect of different additives in a particular polymeric matrix. For example, weathering, environ-

mental degradation, and the thermal stabilization of polymers have been given much attention for many years. Carbon black (CB) has been used as an economical additive in many thermo-plastics and thermosets compounds; it is also a very effective additive for improvement of the outdoor stability of plastics. It has been shown that for high density polyethylene-CB (HDPE) composites, even at a level of 0.05 wt % of CB, the composite has very good UV-screening strength and this can be enhanced further by adding up to 5 wt % of CB.^{6,7} The drawback is, however, that CB can reduce the mechanical properties of HDPE at higher loadings.⁸ It has been shown that the tensile strength of HDPE is increased by addition of up to 3 wt % CB, but higher loadings of up to 8 wt % will not have this effect.⁸

Talc is a mineral composed of hydrated magnesium silicate arranged in three disc-shape layers. In the middle, there is a layer of magnesium-oxygen/hydroxyl octahedra, while the two outer layers are composed of silicon-oxygen tetrahedra. These layers are kept together only by van der Waals' forces, and the layers have the ability to slip over each other easily, which makes talc the softest known mineral, measured as 1 on the Mohs hardness scale.^{9,10} Thanks to its unique characteristics such as softness, chemical inertness, slipping, oil and grease

absorption, whiteness, availability, and its rather low price, talc has been used for many years as an attractive filler in a wide range of industries such as paper, pharmaceuticals, polymers, paint, lubricants, ceramics, and cosmetics.¹¹ In recent years, there has been interest in investigating the effect of talc in polypropylene (PP) blends—not only as filler because of financial considerations but also due to some of its functional properties. Thus, there have been several studies on the influence of talc on the mechanical properties, crystallinity, thermal stability, and crystallite nucleation of PP/talc blends.^{12–16}

Conversely, the most commonly used plastics, such as polyethylene (PE) and PP, are considered to be thermal insulators with low thermal conductivity. There are many new applications such as electronic packaging, pipe networks, heat exchangers, and domestic appliances, in which an increase in the heat transfer properties would be an advantage. There have been many reports on enhancement of the thermal conductivity of polymer composites by addition of different particles, especially metallic and metallic oxides fillers.^{4,17–21} A great number of research papers and reviews have been published, and in many cases they have attempted to introduce models to predict the thermal conductivity of composites according to variables such as thermal conductivity of the matrix, and the thermal conductivity, size, shape, and loading of the filler.^{22–25} A comprehensive review of the various theories and models that have been developed to explain the thermal conductivity of heterogeneous two-phase systems has been written by Bigg.²² Sofian et al.²⁶ studied the thermal conductivity of copper, zinc, iron, and bronze powders in PE matrix. The results showed that the thermal conductivity of the aforementioned composites at a loading of 16 vol % was 1.1, 0.9, 1.3, and 1.8 W/m K respectively. Also, in several papers Tavman^{18,19,27} have investigated the effect of metal particles such as tin, copper, and aluminium on the thermal conductivity of HDPE, and for these fillers the maximum thermal conductivity (3.5 W/m K) was reported for HDPE/aluminium blends to be 33 vol %. These results show that although metal particles have a thermal conductivity several times higher than plastics, the corresponding composites do not have as high values as would be expected. Bigg²² showed that inorganic fillers are as effective in increasing the thermal conductivity as metals, and in this case it is possible to have a combination of good thermal and mechanical properties.

In recent studies, workers have concentrated on studying the effect of single fillers on heat transfer and mechanical properties.^{28–30} However, it could be more promising to study combinations of different fillers, to investigate possible synergetic effects, and also to achieve a balance in thermal conductivity without sacrificing the mechanical properties.

In this study, HDPE precompounded with 2.5 wt % CB was blended in a compounder with up to 35 wt % talc loadings. Specimens were then made by injection moulding for testing of the thermo-physical and mechanical properties. The mechanical properties of the composites were studied by tensile testing and by impact testing. The thermal conductivity, thermal diffusivity, and specific heat were evaluated by the transient plane source (TPS) method, and the thermal stability of blends was examined by thermal gravimetric analysis (TGA). The specific den-

Table I. Characterization of the Compounds Studied

Compound's name	HDPE loading wt %	CB loading wt %	Talc loading wt %	Talc loading v %
PE _n	100	0	0	0
PE _c	97.6	2.4	0	0
5	92.7	2.3	5	1.8
8	89.8	2.2	8	2.9
12	85.9	2.1	12	4.5
15	83.0	2.0	15	5.7
25	73.2	1.8	25	10.2
35	63.4	1.6	35	15.6

sity and long-term water absorption characteristics and morphology were also measured and analyzed.

EXPERIMENTAL

Materials

High-density polyethylene (HDPE) was used as a matrix material, which was supplied by Unipetrol RPA, Czech-Republic. The HDPE has a melt flow rate (MFI) of 0.4 g/10 min, a Vicat softening temperature of 118°C, and a density of 952 kg/m³. This polyolefin contains 2.5 wt % of CB, which was fully precompounded by the supplier. For simplicity, from here onward the material is referred to as “PE_c” (HDPE with CB). In order to investigate the effect of this amount of CB, a sample of the same neat HDPE resin without CB was also obtained from the same supplier, and this material is referred to as “PE_n” (HDPE neat). The neat HDPE has an MFI of 0.4 g/10 min, a Vicat softening temperature of 122°C, and a density of 942 kg/m³. The PE_n was used as a reference to investigate the effect of the CB added on the neat HDPE, and the PE_c was used as a reference to study the effect of talc on the HDPE/CB/talc composites (The above information for PE_c and PE_n were given by supplier). Commercial talc HAR T84 from Luzenac, France, was used as filler in this study.

Particle Size Distribution of Talc

The particle size distribution was determined with a Malvern Mastersizer, which can determine particle sizes in the range 0.05–1000 μm. Hundred milliliter of deionized water was used as the particle dispersant. To prevent poor dispersion in the dispersant, about 20 mg of the talc was put in a glass test tube and then 3 mL of deionized water was added. The sample was then treated in an ultrasonic bath for 5 min to break up agglomerates. The thoroughly dispersed suspension was then transferred to the Mastersizer and measured. During the measurement, the sample was agitated in the cell to avoid any settling of the particles. Duplicate measurements of each sample were performed and the average value is reported, together with standard deviation.

Preparation of Composites

Composites were prepared by compounding the PE_c and the talc at different ratios according to Table I, in a twin-screw extruder with two side-feeders (ZSK 25 WLE; Cooperion Werner & Pfleiderer, Germany). The temperature profile used was 180–

220°C from feed to die (above the melting temperature of HDPE and well below its decomposition temperature). The PEC was fed into the main hopper with a screw speed of 230 rpm while the talc was fed into the side-feeder with a screw speed of 300 rpm. Two individually controlled gravimetric K-tron feeders were used to control the feeding rate, both for the resin and the filler. The throughput was set to 13.67 kg/h for the main feeder, while the throughput for the side-feeder was set to obtain the desired sample composition. The extruded strand was cooled in a water bath and pelletized. The granules were then oven-dried followed by injection moulding in an Engel ES 200/110HL Victory with a screw diameter of 30 mm into tensile-testing bars according to ISO standard 572-2/1A. These test bars were also used for the Charpy impact resistance measurement, thermal conductivity measurements, and water absorption testing. For these tests, the samples were cut to the exact dimensions according to the test standards.

Thermogravimetric Analysis

The thermogravimetric analysis was done in a TA instrument Q 500 TGA supplied by Waters LLC, New Castle, IN. Samples of 15 ± 3 mg were heated at $10^\circ\text{C}/\text{min}$ in a nitrogen purge stream from 30 to 800°C . The flow rate of the nitrogen stream was 50 mL/min. The samples were first heated up in a nitrogen atmosphere to 600°C and then the gas was switched to oxygen until 800°C . The weight change as a function of time was recorded and analyzed. The flow rate for both nitrogen and oxygen was 50 mL/min.

Mechanical Testing

The tensile testing was performed according to ISO 527 with a tensile-testing machine MTS 20/M with a cross-head speed of 50 mm/min. Dog-bone samples for mechanical testing were prepared as described in the previous section. The samples had a gauge length of 50 mm, a thickness of 4 mm, and a width of 10 mm. Young's modulus was determined as the tangent of the initial elastic region. At least six samples were tested for each composition, and their averages are shown with standard deviation bars.

The Charpy impact strength was done according to ISO 179-1 with a Zwick test instrument (Zwick GmbH, Ulm, Germany). A total of 10 specimens for each composition (80-mm long, 10-mm wide, and 4-mm thick) were tested to determine the mean impact resistance. The samples were cut from the tensile-testing specimens. The sample designations are ISO 179-1/1eA for specimens that were tested notched and edgewise and ISO 179-1/1fU for those tested unnotched and flatwise.

Thermal Conductivity

Simultaneous measurements of the thermal conductivity, thermal diffusivity, and volumetric specific heat of all composites were done at room temperature and under normal pressure by the hot disk TPS (TPS 2500 Gothenburg, Sweden) according to ISO 22007-2.2. A 4-mm diameter Kapton sensor disk was used to do the measurement at room temperature. The sample size was $50 \times 10 \text{ mm}^2$ and the thickness was approximately 4 mm. Samples were cut from the tensile bar specimens. Since the test was carried out at ambient temperature, a fixture had been constructed in order not to interfere with other external source of

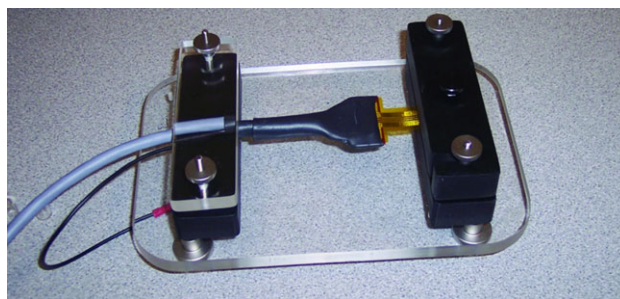


Figure 1. Fixture for the thermal conductivity measurement. [Color figure can be viewed in the online issue, which is available at wileyonlinelibrary.com.]

heat (Figure 1). In the fixture, two identical samples were used in each measurement; one sample was placed beneath the sensor and the other was placed on top, of the sensor. The fixture was equipped with a heat source to enable sample heating. Data were collected from both samples at the same time, and the software reported thermal properties as the average value of both samples. Each measurement was done at three different positions on the sample surface, and the average of these values is reported. Then the specific heat C_p of the samples was calculated by dividing the measured volumetric heat capacity by the measured specific density.

Density

The specimens were characterized regarding dimensional stability by determining the specific density according to the Archimedes method as described by ASTM D792 test method B. This involves the measurement of the volume from the buoyancy in a fluid of known density. A Kern analytical balance with a precision of 0.0001 g was used for all weight measurements. The samples were weighed in air (A), as well as in medium (B), which had a known density (ρ_0) at room temperature. The specific density of the composite (ρ) was then calculated as follows:

$$\rho = \frac{A}{A - B} \rho_0$$

Ethyl alcohol, which has a density of $0.78860 \text{ g}/\text{cm}^3$ at 21°C , was chosen as the fluid.

Moisture Absorption

Water absorption analysis was done on selected composite specimens according to ASTM D570-98. The test specimens were cut into the dimensions of 30-mm long, 10-mm wide, and 4-mm thick from the tensile bars prepared as described earlier. The specimens were dried for 24 h at 60°C and cooled to room temperature in a desiccator. They were weighed to the nearest 0.0001 g (W_0). The test specimens were then immersed for 24 h in distilled water at room temperature ($22 \pm 1^\circ\text{C}$). After this time, they were removed from the water and their surfaces were wiped dry. They were then weighed (W_1), and placed back in the distilled water. Three specimens were analyzed for each of the selected compositions and the average was calculated. The percentage of water absorption (WA%) was calculated using the equation:

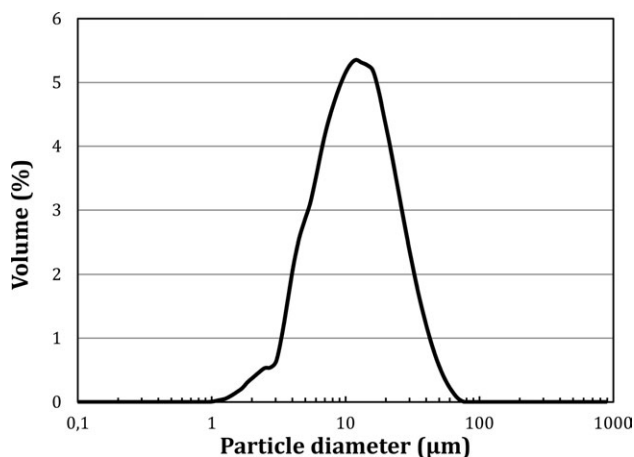


Figure 2. Particle size distribution.

$$WA\% = (W_1 - W_0) \times 100/W_0$$

Here, W_0 is the conditioned weight after drying and W_1 is the weight after immersion in water. The procedure was done every second week, until it resulted in an increase in weight of less than 1%.

Scanning Electron Microscopy (SEM)

The cross-sectional fracture surfaces of the specimens were studied by SEM, using a JEOL model JSM-6610LV scanning electron microscope (JEOL Ltd, Akishima, Japan). The tensile bar specimens were fractured after immersion in liquid nitrogen, to create a brittle fracture.

Statistical Analysis

Statistical comparisons, based on one-way analysis of variance (ANOVA) at the 95% confidence level, were performed to test the effects of the filler and their interactions on the mechanical properties. Analysis of data was done using Minitab (version 15).

RESULTS AND DISCUSSION

Particle Size

Figure 2 shows the particle size distributions with respect to the cumulative volume and the volume in each size fraction. The values $D(10)$, $D(50)$, and $D(90)$ indicate that 10, 50, or 90%

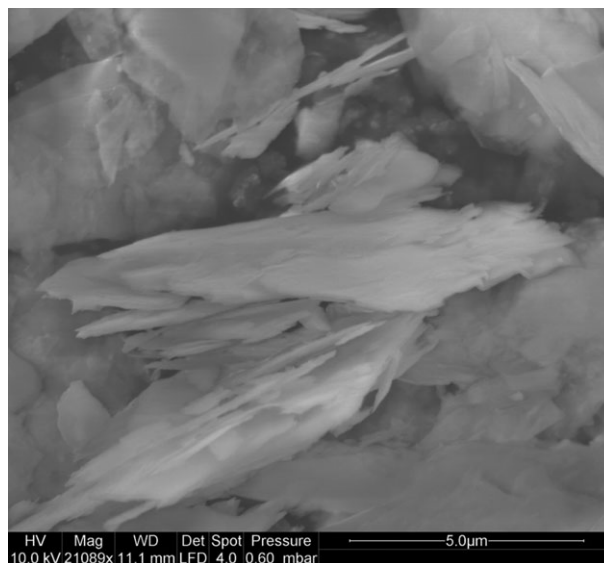


Figure 3. Micrograph of a talc particle.

(by volume) of particles have a size equal to or less than that corresponding value. The mean particle size was $11.14 \pm 0.02 \mu\text{m}$. Figure 3 is a micrograph of the talc before compounding, in which the plate-like shape of the particles can be seen clearly. From the micrograph, the length of particulates were measured by image analysis, and the median diameter obtained ($10.2 \mu\text{m}$), was in good agreement with the result from the MasterSizer method.

Mechanical Properties

Table II shows the influence of the talc loadings on the tensile strength, elongation at yield, and elongation at break, as well as the E-modulus. Figure 4 shows the individual broken specimens after the tensile test, and it can be seen that whitening occurred only for the PEn sample, while the rest of the samples had a ductile failure with necking of the specimen. From Figure 5, one can see that the tensile strength at yield increased gradually with increasing filler content. In contrast, PE_c, which had 2.5% CB, showed a slight decrease in tensile strength compared to HDPE with no filler (PEn). The increase in tensile strength on incorporation of talc was more evident at higher concentrations. To evaluate the significance of differences observed between different composite formulations, the data (for the six talc

Table II. Mechanical Properties of the Different Composites (Uncertainties Represent the Standard Deviation)

Blend	Strain at yield %	Stress at yield MPa	Stress at braek MPa	E-Modulus MPa
PE _n	22 ± 1.9	26 ± 0.3	13.3 ± 0.2	660.5 ± 16.8
PE _c	20.4 ± 1.1	25.1 ± 0.5	13.1 ± 0.2	695.8 ± 20.0
5	16.9 ± 2.4	24.5 ± 0.1	12.3 ± 0.1	774.2 ± 31.1
8	20.9 ± 1.1	24.6 ± 0.1	12.3 ± 0.0	988.3 ± 18.9
12	15.1 ± 0.7	25.3 ± 0.2	12.7 ± 0.1	1,057.9 ± 57.9
15	12.9 ± 0.7	25.8 ± 0.1	12.9 ± 0.1	1,201.8 ± 15.4
25	9.7 ± 0.9	26.5 ± 0.3	13.3 ± 0.1	1,680.9 ± 51.7
35	7.1 ± 0.5	28.6 ± 0.2	14.3 ± 0.1	2,231.1 ± 38.7



Figure 4. Individual test specimens after the tensile test. [Color figure can be viewed in the online issue, which is available at wileyonlinelibrary.com.]

concentrations from 5 to 35% and PE_c as control) were analyzed by one-way ANOVA at the 95% confidence level. A *P*-value for the tensile strength at yield was less than $\alpha = 0.05$, we concluded that the effect was statistically significant. The same result was obtained for the tensile strength at break, also shown in Figure 5. The *P*-value of < 0.05 for the tensile strength at break indicated that there were significant differences between the various composites. Regarding the elongation at yield, as anticipated, the PE_n (pure HDPE) had the highest value of all compounds. Generally, a decrease in elongation with an increase in filler content can always be expected due to the fact that the filler added causes a reduction in chain mobility, giving rise to a rapidly decreasing elongation at break. However all the compounds (except PE_c with 8% talc) showed a decrease in strain at yield. The stiffness was increased with both fillers: in the presence of CB, the E-modulus showed a slight increment—about 5% compared to HDPE without filler—whereas the role of talc was more prominent. Despite the fact that the two additives CB and talc are totally different in terms of shape and size,

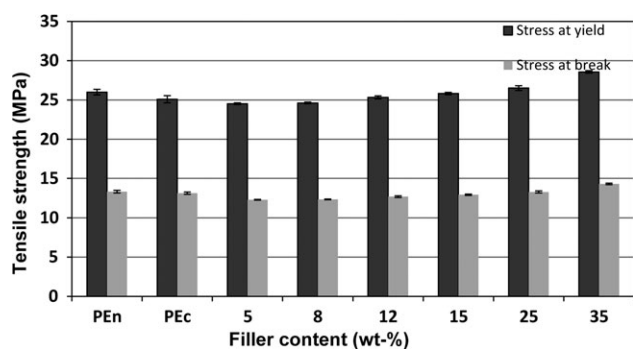


Figure 5. Tensile strength at yield and break.

the tensile modulus increased with higher content of either type of particle. This behavior has been discussed by Leong et al.³¹ and Bakar et al.³² They reported that as the Young modulus is measured in the elastic area before any major plastic deformations occur, improvement in the stiffness is more due to the fact that rigid particulates restrict the mobility of the chain segments of the macromolecule. Thus, improvement in the stiffness of composites is only weakly dependent on particle size and shape. However, Busigin et al.³³ have shown that the stiffness should show an increase as the flake aspect ratio increases, but for particles with aspect ratio greater than $100 \mu\text{m}$ there is a tendency to break down during processing. They have also shown that for two very similar particles like mica and talc at same concentration with PP, mica is twice as effective respect to modulus. Based on the above considerations and also our observations on the micrographs, we attribute improvement of the modulus to the dispersion of the filler in the samples we

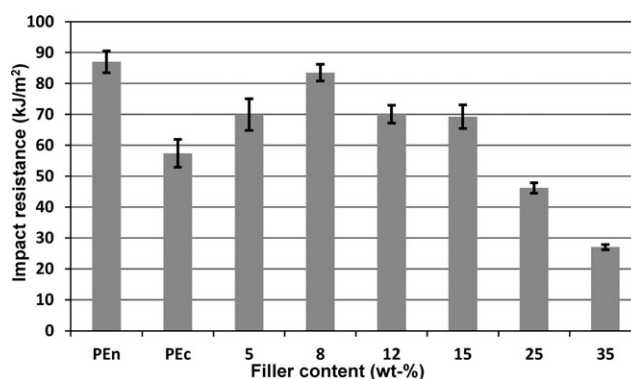


Figure 6. Impact resistance as a function of talc filler (notched and edgewise).

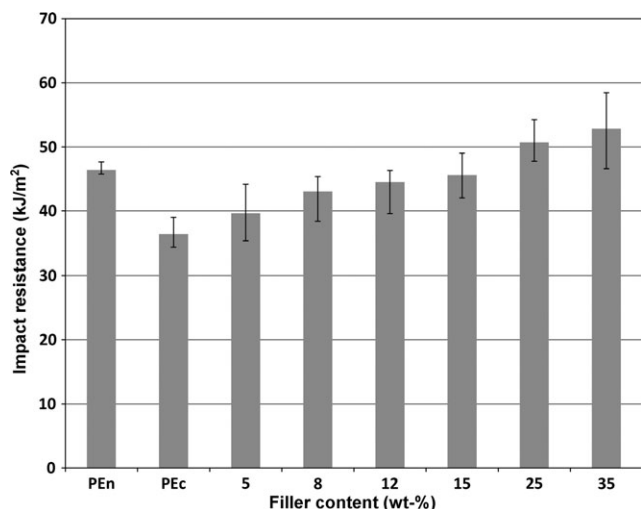


Figure 7. Impact resistance as a function of talc filler (unnotched and flatwise).

studied. To a certain degree, the stiffness of the composites relies on the uniform dispersion of the particle in the matrix. It is usually expected that agglomerates are formed when the particle amount is increased, leading to decrease in modulus. But in our case, the modulus increased even at the highest talc concentration. This led us to infer that the talc particles are distributed uniformly but not randomly, and not as aggregates, even at the highest concentration. This will be discussed later in this section.

The variation in the impact strength with filler concentration is illustrated in Figures 6 and 7 for notched specimens in the edgewise direction respective unnotched specimens in the flatwise direction. As expected, almost the same behavior was detected for the Charpy impact resistance (notched specimen, edgewise direction) and the tensile elongation (Figure 8). At first, with incorporation of 2.5 wt % of CB in the HDPE, the toughness was steeply reduced by 34%. Then, in the presence of

talc, the toughness gradually improved until at 8 wt % loading the highest value for impact was reached, which was very close to the value for pure HDPE (83 kJ/m²). After that, the impact resistance dropped gradually with an increase in filler loading. As some materials and composites are more sensitive to notches than others, it is advisable to compare the results for notched and unnotched specimens.³⁴ The Charpy impact test was also done with unnotched, flatwise direction and the results are shown in Figure 7. In the recent case also, the same trend can be noted that PEc showed a moderate drop in impact resistance compared to PEn (as for the notched, edgewise case). With increase in talc loading, the impact strength increased.

Statistical analysis using one-way ANOVA also gave a significant effectiveness of talc on the impact strength compared to the PEc for both impact directions. Further the ANOVA analysis according to Hsu's MCB method (multiple comparisons with the best) showed that the composite with 8 wt % talc was the best of all with 95% confidence interval.

The interpretation of the mechanical properties is supported by the SEM micrographs. Figures 9–11 show micrographs of the cryo-fractured surfaces of PEc and of composites with 8, 25, and 35 wt % talc. It is clear that the filler is well dispersed and uniformly distributed in the matrix. Also, the layers of talc, which are held together by weak van der Waals' forces, are oriented along the direction of injection flow. This organization of particles is a result of the plate-like structure of talc with its high aspect ratio, as the layers of talc can easily slip over each other during the injection moulding. Finally, the polymer can easily fill the spaces between the particles. From these SEM images, it can be seen that the parts of the filler that were protruding from the surface appear to lack remnants and residues of matrix, which would have been the case if the adhesion was good. In Figure 11, pull-out of talc particles can be seen from the imprints left on the surface. The dimensions of the imprints are in quite good agreement with the size measured for talc. On these grounds, we could conclude that the adhesion between

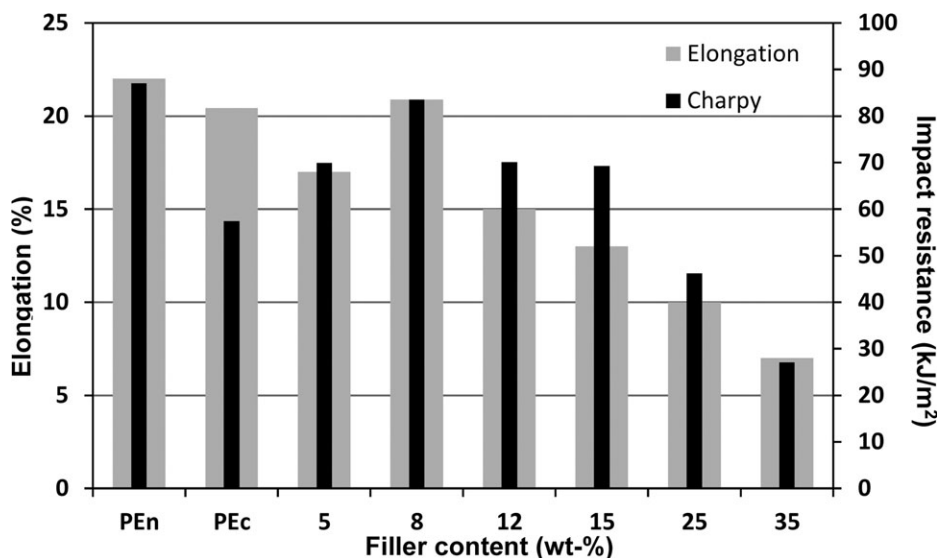


Figure 8. Elongation at yield and Charpy impact resistance of the composites.

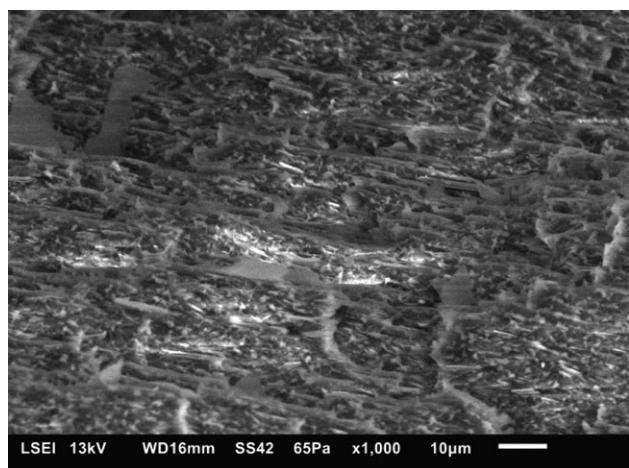


Figure 9. SEM micrographs of the cryo-fractured surfaces of PEC/talc (8 wt %).

talc and matrix in this system was poor, which explains why the tensile strength did not increase very much.

It is generally known that a lower filler-matrix adhesion results in better impact resistance.^{8,34,35} The results obtained indicate that adhesion between the CB particles and the HDPE matrix is better than between the talc and the matrix. This was evident both in flatwise and edgewise impact testing. Since the talc layers are kept together only by weak van der Waals' forces, the layers can slip easily, but when the external load is applied in the direction perpendicular to the particle orientation (flatwise), the talc particles are more able to take up the external load. However, the dispersion of filler in all blends showed that there was no severe agglomeration of particles, which confirms why the stiffness was increased at all proportions of talc.

It is known that talc is a strong nucleating agent for polymer crystallization, which can also cause changes in the mechanical properties. A detailed study of the crystallinity and morphology of these blends is in progress, to gain a more complete under-

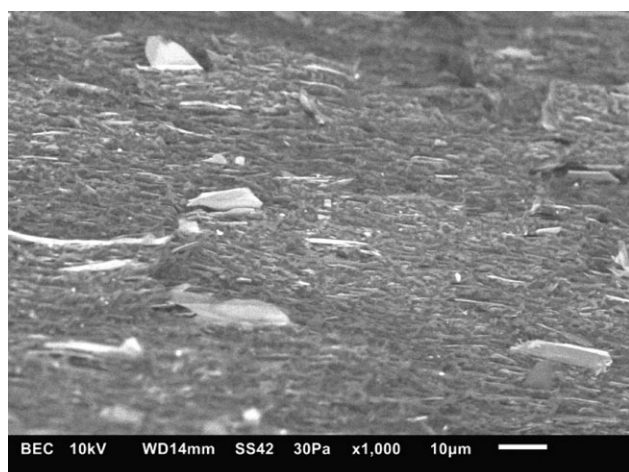


Figure 10. SEM micrographs of the cryo-fractured surfaces of PEC/talc (25 wt %).

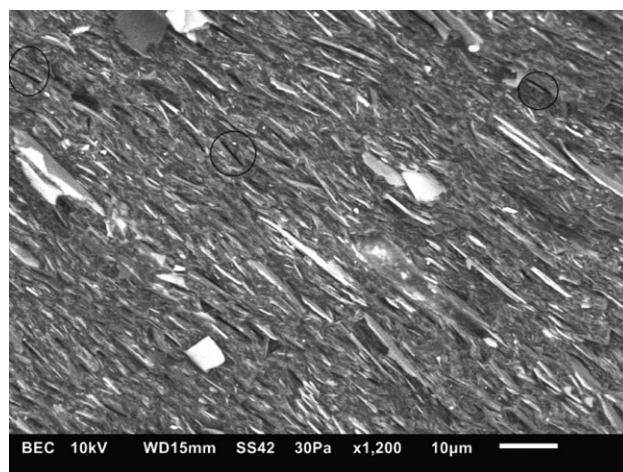


Figure 11. SEM micrographs of the cryo-fractured surfaces of PEC/talc (35 wt %).

standing of the structure, and the results will be reported in later studies.

Thermogravimetric Analysis

Results from the TGA measurements are shown in Figure 12 and summarized in Table III. It was found that the PEN started to degrade at a temperature of 395°C, and decomposition of almost 100% occurred at 570°C. It was also found that the thermal stability of PEC was more pronounced than for the PEN (Figure 13): a decomposition of PEN of 5% occurred at 395°C while 5% degradation in weight for PEC occurred at 435°C. Additionally, the maximum mass loss temperatures were 448°C and 462°C, respectively. One explanation for the higher thermal stability for PEC might be the moderate enhancement of the thermal conductivity and the uniform heat dissipation. Apart from that, CB has a nonpolar surface character, which is more compatible in a matrix like HDPE, as it is also nonpolar.³⁶ Thus, the interfacial heat transfer could be improved, reducing local overheating and hot spots, which can delay the thermal degradation.^{17,20} The effect of CB on the thermal stability of different polymers has been reported by Jakab and co-workers,^{37,38} and they showed that the thermal decomposition of PE is hindered in the presence of CB if it is in good physical contact with the matrix. As mentioned earlier, the presence of CB can have a positive effect on the light stability and protection against UV, which shows that CB can also be considered to be a thermal stabilizer in this case. The thermal stability of the composites of talc and PEC did not show any improvement over that of PEC: even at higher talc concentrations, the initial decomposition temperature was lower than for neat PEN. The mechanism of accelerated degradation can be explained in two ways. First, the ability of the talc particle surface to absorb stabilizers can result in reduced long-term thermal stability. Therefore, as the specific surface area of the filler is increased, this adverse effect can be more pronounced.³⁹ The second reason could be impurities in the talc, e.g. traces of heavy metals. Heavy metal ions such as copper, cobalt, manganese, or iron—if present—can catalyze the degradation.⁴⁰ Other studies have shown that the degradation of PP/talc compounds by sunlight

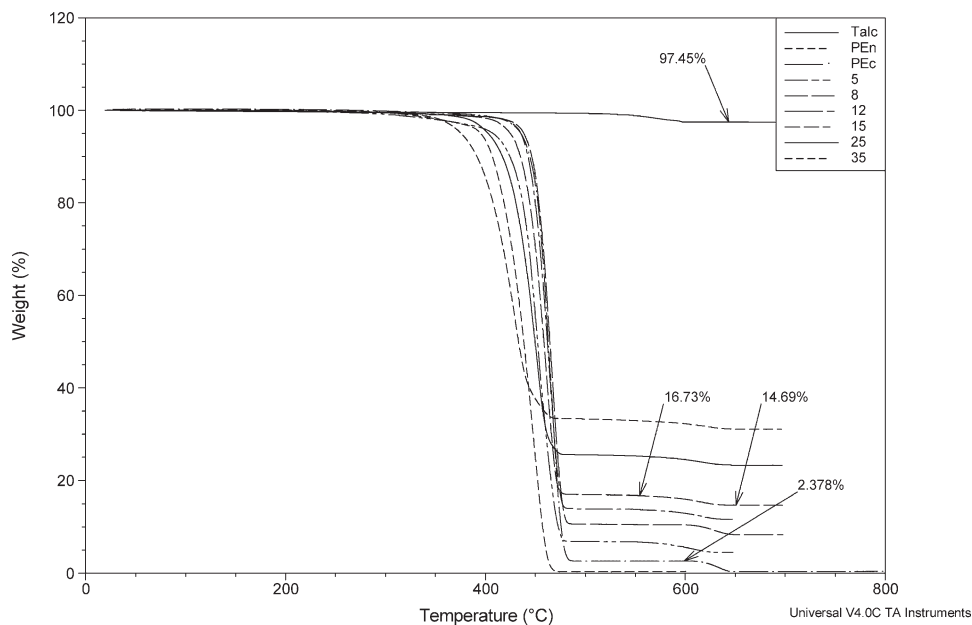


Figure 12. TGA of PEn and PEc with different talc concentrations.

Table III. Thermal Degradation and Residue for Individual Samples

Material properties	Talc	PE _n	PE _c	5	8	12	15	25	35
Temperature for 5 wt % loss (°C)	-	395	435	408	438	435	425	402	376
Temperature for max weight loss (°C)	569	448	462	453	466	464	461	452	430
Residue at 550°C (%)	98.85	0.3	2.36	6.78	10.52	13.76	16.78	25.29	32.97
Residue at 650°C (%)	97.44	0.3	0.1	4.45	8.33	11.63	14.69	23.32	31.12

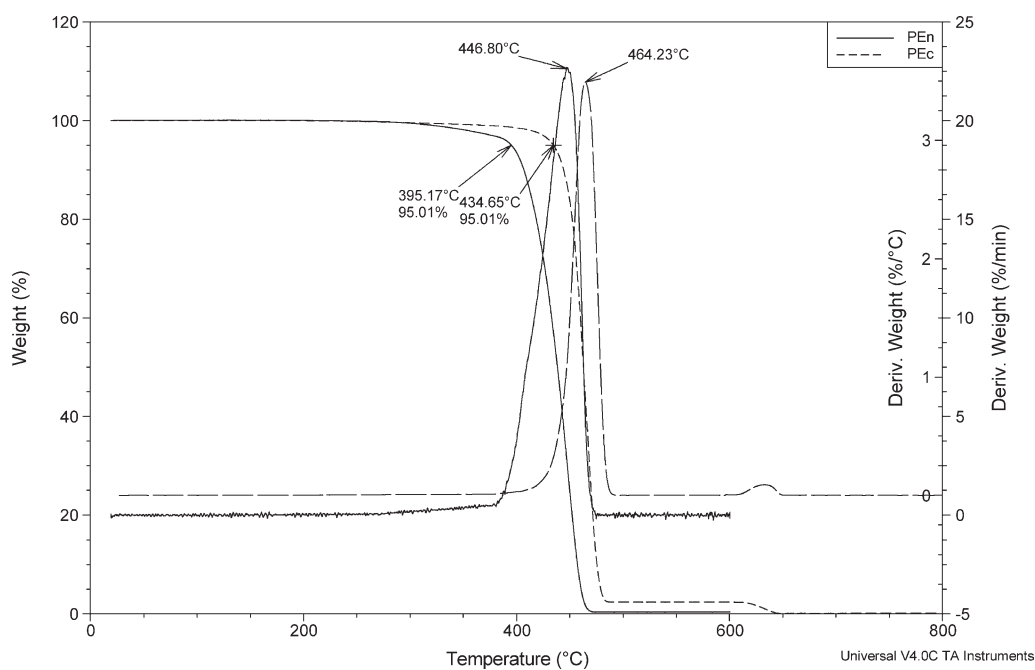


Figure 13. Thermogravimetric traces of PEn and PEc.

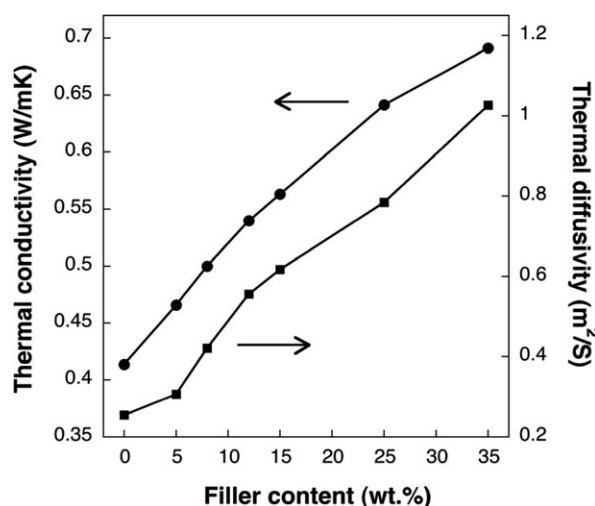


Figure 14. Thermal conductivity and thermal diffusivity of samples.

can also be accelerated synergistically with loading of the talc.^{41,42} There have also been other studies in the same area showing that PP/talc has lower UV- and long-term thermal stability.^{16,43} Figure 13 shows that the mass loss for pure talc in the interval from room temperature up to 800°C was about 2.5%. This indicates that it is quite stable. The weight loss was a little higher than the value given by the supplier while the onset temperature for the pure talc decomposition occurred below 650°C, which is slightly lower than the value given in the literature.³⁹

Table III also shows that almost 100% of the PE in all samples degraded at 550°C, and that the residue contained CB and talc. When the inert gas was switched to oxygen at 600°C, the CB became oxidized, which left the talc as a residue. The amount of CB can therefore be calculated by subtracting the weight loss at 650°C from that at 600°C. The amount of final residue increased correspondingly with the proportion of filler. The calculated percentage of residue for CB and talc for each composite was in accordance with the values given in Table I.

Thermal Conductivity

Thermal conductivity, thermal diffusivity, and heat capacity of the samples investigated (except for PEn) are plotted in Figures

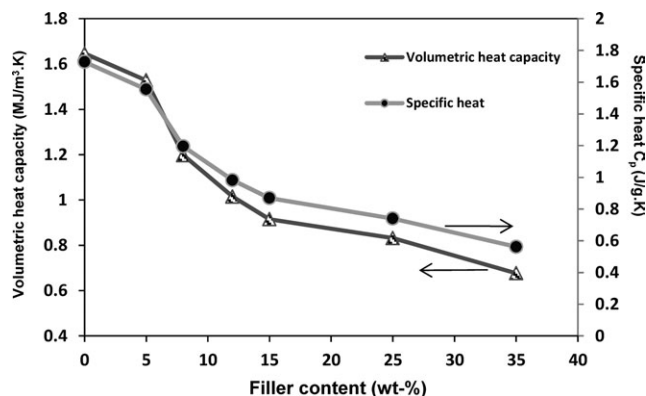


Figure 15. Volumetric heat capacity and specific heat as a function of filler content.

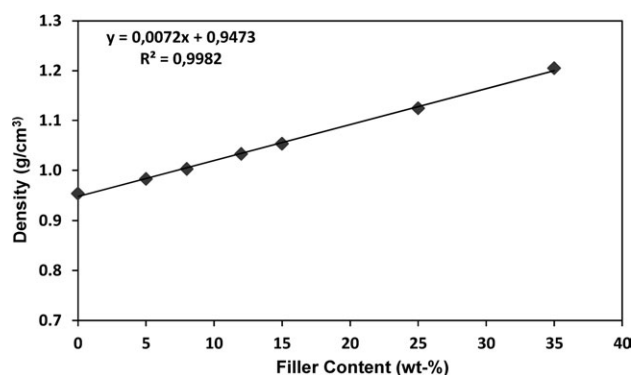


Figure 16. Long-term effects of water absorption on different filler content.

14 and 15. It was found that the thermal conductivity and the thermal diffusivity increased gradually, and both volumetric and specific heat capacity (C_p) decreased with the talc increment. It should be noted that the specific heat capacity of talc is about 50% of the value for PEc, so a decrease in C_p for the composites with talc loading could be expected. From the application point of view, this means that improving heat transfer in the melt by introducing talc particles leads to a faster production rate, which would be important in terms of production output and cycle time. The enhancement of the thermal conductivity indicates that a percolated particle network was not formed, as we could not achieve the thermal conductivity values of pure talc. At higher filler concentrations, one would expect that the fillers would form thermally conductive percolated networks (instead of isolated thermally conductive particles surrounded by the matrix), and heat can therefore flow through these channels. The maximum thermal conductivity was up to 70% higher than for unfilled PEc at a talc concentration of 35 wt %. As discussed previously regarding the mechanical properties and as illustrated in Figures 9–11, the talc particles were well dispersed throughout the matrix, and the particles could not form a percolated conductive path. So these results show that the heat transfer occurred according to the dispersion mechanism, with no percolation, as has been reported in the literature for other fillers.^{18,23} Moreover, Weidenfeller et al.⁴⁴ studied the thermal conductivity of different particulates in a PP matrix and showed that although copper (Cu) has a thermal conductivity that is about 20 times higher than for talc, the thermal conductivity of the PP/talc composites had a higher value than that of PP/Cu when compared at the same volume fractions (from 0–30%). They concluded that the interconnectivity of the filler and matrix is the key factor for thermal conductivity of the composites.⁴⁴ The value measured for the thermal conductivity of PEc/talc was lower than that measured for PP/talc in the study by Weidenfeller et al.

Water Absorption and Density

The dependencies of specific density with weight fraction of filler is illustrated in Figure 16 (the value for the density of PEn is not shown). Table IV shows a summary of the short- and long-term water uptake. Both water absorption and the density of composites increased with increased filler content in the blend.

Table IV. Short-Term and Long-Term Water Absorption of the Compounds (Uncertainties Represent the Standard Deviation)

Compound	PE _n	PE _c	5	8	12	15	25	35
Water absorbed								
After one day (%)	0.027 ± 0.04	0.012 ± 0.01	0.014 ± 0.02	0.02 ± 0.02	0.016 ± 0.01	0.011 ± 0.02	0.015 ± 0.02	0.014 ± 0.01
After one week (%)	0.021 ± 0.01	0.074 ± 0.02	0.063 ± 0.02	0.071 ± 0.02	0.065 ± 0.02	0.054 ± 0.02	0.066 ± 0.02	0.076 ± 0.01
After 14 weeks (%)	0.057 ± 0.00	0.091 ± 0.01	0.124 ± 0.00	0.125 ± 0.02	0.142 ± 0.02	0.143 ± 0.00	0.18 ± 0.01	0.206 ± 0.01
After 22 weeks (%)	0.045 ± 0.02	0.083 ± 0.02	0.135 ± 0.04	0.139 ± 0.01	0.15 ± 0.01	0.146 ± 0.01	0.182 ± 0.01	0.224 ± 0.01

Nevertheless, while the increment of density was linearly proportional to the talc content, the curve corresponding to water absorption showed a nonlinear relationship with time. As shown in Figure 16, both fillers caused the water retention to increase and the general trend was that as the loading increased, the sample under study exhibited higher water absorption. This rate was high in the beginning and after a week the weight increase became quite stable. For the PE_n and PE_c samples the moisture absorption did not increase after 2 weeks, due to saturation. For all talc-filled samples the overall water absorption was unremarkable (at 0.2% for the highest value) after 8 weeks.

The experimental values for density were in good agreement with the theoretical values obtained by the rule of mixtures.

CONCLUSIONS

The mechanical and thermo-physical properties of HDPE-talc-CB composites were investigated. CB proved to be an effective additive for enhancement of thermal stability, while it had a negative effect on the mechanical properties, particularly impact resistance. We have emphasized that due to its plate-like shape and as it has a aspect ratio according to the SEM analysis, talc is a promising particulate to enhance the impact strength and the thermo-physical characteristics of PE. The improvement in toughness perpendicular to the direction of flow was more pronounced, while the tensile at break and yield tensile remained unchanged when increasing talc addition. The thermal conductivity, the thermal diffusivity, and the specific density of the composites were enhanced, while the specific heat capacity of the composites decreased, which can increase production speed.

ACKNOWLEDGMENTS

The authors are grateful to the Muovitech International Group in Borås, Sweden, for their financial support for this research study.

REFERENCES

- Alter, H. J. *Appl. Poly. Sci.* **1965**, *9*, 1525.
- Gao, Z.; Tsou, A. H. *J. Polym. Sci. Part B: Polym. Phys.* **1999**, *37*, 155.
- Mamunya, Y. P.; Davydenko, V. V.; Pissis, P.; Lebedev, E. V. *Eur. Polym. J.* **2002**, *38*, 1887.
- Bigg, D. M. *Polym. Eng. Sci.* **1979**, *19*, 1188.
- Ammala, A.; Hill, A. J.; Meakin, P.; Pas, S. J.; Turney, T. W. *J. Nanopart. Res.* **2002**, *4*, 167.
- Bigger, S.; Delatycki, O. *J. Mater. Sci.* **1989**, *24*, 1946.
- White, J. R.; and Turnbull, A. *J. Mater. Sci.* **1994**, *29*, 584.
- Liang, J. Z.; Yang, Q. Q. *J. Reinforced Plastics Compos.* **2009**, *28*, 295.
- Du, H.; Miller, J. D. *Int. J. Miner. Process.* **2007**, *84*, 172.
- Suh, C. H.; White, J. L. *J. Non-Newtonian Fluid Mech.* **1996**, *62*, 175.
- Ulusoy, U. *Powder Technol.* **2008**, *188*, 133.
- Da Silva A. L. N.; Rocha, M. C. G.; Moraes, M. A. R; Valente, C. A. R; Coutinho, F. M. B; *Polym. Test.* **2002**, *21*, 57.

13. McGenity, P. M.; Hooper, J. J.; Paynter, C. D.; Riley, A. M.; Nutbeam, C.; Elton, N. J.; Adams, J. M. *Polymer* **1992**, *33*, 5215.
14. Choi, W. J.; Kim, S. C. *Polymer* **2004**, *45*, 2393.
15. Denac, M.; Musil, V.; Šmit, I.; Ranogajec, F. *Polym. Degrad. Stab.* **2003**, *82*, 263.
16. Rotzinger, B. *Polym. Degrad. Stab.* **2006**, *91*, 2884.
17. Maiti, S. N.; Mahapatro, P. K. *Polym. Compos.* **1990**, *11*, 223.
18. Tavman, I. H.; *J. Appl. Polym. Sci.* **1996**, *62*, 2161.
19. Tavman, I. H. *Powder Technol.* **1997**, *91*, 63.
20. Maiti, S. N.; Ghosh, K. *J. Appl. Polym. Sci.* **1994**, *52*, 1091.
21. Herschel, W. G.; Waldemar, T. Z. *J. Appl. Phys.* **1966**, *37*, 56.
22. Bigg, D., *Adv. Polym. Sci.*, **1995**, *119*, 1.
23. Agari, Y.; Uno, T. *J. Appl. Polym. Sci.* **1985**, *30*, 2225.
24. He, H.; Fu, R.; Han, Y.; Shen, Y.; Song, X. *J. Mater. Sci.* **2007**, *42*, 6749.
25. Liang, J.; Liu, G. *J. Mater. Sci.* **2009**, *44*, 4715.
26. Sofian, N. M.; Rusu, M.; Neagu, R.; Neagu, E. *J. Thermoplast. Compos. Mater.* **2001**, *14*, 20.
27. Tavman, I. H. *Int. Commun. Heat Mass Transfer* **1998**, *25*, 723.
28. Zhou, W.; Qi, S.; An, Q.; Zhao, H.; Liu, N. *Mater. Res. Bull.* **2007**, *42*, 1863.
29. Krupa, I.; Boudenne, A.; Ibos, L. *Eur. Polym. J.* **2007**, *43*, 2443.
30. Järvelä, P. A.; Järvelä, P. K. *J. Mater. Sci.* **1996**, *31*, 3853.
31. Leong, Y. W.; Abu Bakar, M. B.; Ishak, Z. A. M.; Ariffin, A.; Pukanszky, B. *J. Appl. Polym. Sci.* **2004**, *91*, 3315.
32. Bakar, M. B. A.; Leong, Y. W.; Ariffin, A.; Ishak, Z. A. M. *J. Appl. Polym. Sci.* **2007**, *104*, 434.
33. Busigin, C.; Martinez, G. M.; Woodhams, R. T.; Lahtinen, R. *Polym. Eng. Sci.* **1983**, *23*, 766.
34. Nielsen, L. E. *Mechanical Properties of Polymers and Composites*; Marcel Dekker: New York, **1994**.
35. Thio, Y. S.; Argon, S.; Cohen, R. E. *Polymer* **2004**, *45*, 3139.
36. Wypych, G.; *Handbook of Fillers, 3e*; ChemTec Publishing, Toronto, Canada, **2009**.
37. Jakab, E.; Blazsó, M. *J. Anal. Appl. Pyrolysis*, **2002**, *64*, 263.
38. Jakab, E.; Omastová, M. *J. Anal. Appl. Pyrolysis* **2005**, *74*, 204.
39. Zweifel, H.; Maier, R. D.; Schiller, M. *Plastics Additives Handbook*; Hanser, Munich, Germany, **2009**.
40. Zweifel, H., Maier, R. D., Schiller, M. In *Plastics Additives Handbook*, Hanser, Munich, Germany, **2009**; p 1222.
41. Azuma, Y.; Takeda, H.; Watanabe, S.; Nakatani, H. *Polym. Degrad. Stab.* **2009**, *94*, 2267.
42. Lee, J.-Y.; Shim, M.-J.; Kim, S.-W. *J. Mater. Sci.* **2001**, *36*, 4405.
43. Xingzhou, H.; Hongmei, X.; Zhenfeng, Z. *Polym. Degrad. Stab.* **1994**, *43*, 225.
44. Weidenfeller, B.; Höfer, M.; Schilling, F. R. *Compo. Part A: Appl. Sci. Manufact.* **2004**, *35*, 423.